

Multiple Length Scale Instabilities of Unidirectional Pulse Propagation in a Diffusion-Fed Gel

Xing-Jie Lu,[†] Lin Ren,[†] Qing-Yu Gao,^{*,†} Ying-Ying Yang,[†] Yue-Min Zhao,[†] Jun Huang,[†] Xiao-Li Lv,[†] and Irving R. Epstein^{*,‡}

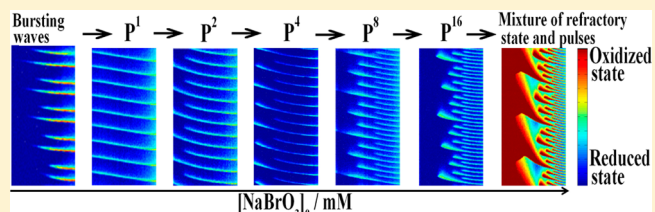
[†]College of Chemical Engineering, China University of Mining and Technology, Xuzhou 221008, China

[‡]Department of Chemistry and Volen Center for Complex Systems, MS 015, Brandeis University, Waltham, Massachusetts 02454-9110, United States

Supporting Information

ABSTRACT: Patterns containing multiple length scales arise in a variety of natural systems such as lateral veins in leaves, fingerprints, wrinkled skin, and dendritic crystals. Here we observe period-doubling and bursting instabilities in the spatial extent of wave propagation in a gel-filled capillary tube open at one end and containing the Belousov–Zhabotinsky (BZ) reaction–diffusion system. We analyze the relationship between the multiple propagation distances of pulse waves and the local kinetics of the reaction–diffusion system. Simulations with a five-variable Oregonator model qualitatively mimic the multiple length scale patterns of pulse propagation observed in our experiments, suggesting that the study of these phenomena in reaction–diffusion systems may be helpful in understanding complex multiple length scale dynamical behaviors in nature.

SECTION: Kinetics and Dynamics



Complex oscillations displaying multiple time scales, such as period-doubling, mixed-mode, and bursting oscillations, which arise from instabilities of simple oscillations in spatially homogeneous systems, have received considerable attention in the literature.^{1–3} Spatial multiple length scale instabilities of propagating waves bifurcating from single length scale (simply periodic in space) waves have been less thoroughly studied. Multiscale growth patterns are ubiquitous in nature, leading to complex structures exquisitely tailored to perform specific functions. Furthermore, in a developing body, growth rates may differ with location and/or time, resulting in multiple scale structures, e.g., growth of lateral veins in leaves,⁴ formation of fingerprints⁵ and wrinkling of skin.⁶ Such growth structures share a common underlying dynamics, i.e., coupling between (physical or chemical) interaction and transport. In plant growth, for example, nutrients are diffusion-fed from the trunk and branches to leaf veins at multiple levels, where biocatalysts then transform nutrients and CO₂ to biomolecules, resulting in new lateral veins with multiple length scales.⁴ Losert et al.⁷ reported spatial period-doubling in the directional solidification of dendritic arrays of acetone-doped succinonitrile in good agreement with the theoretical prediction of Warren and Langer.⁸ Brau et al.⁹ also observed period-doubling behavior during compression of an elastic membrane and analyzed the phenomenon with a nonlinear Euler–Lagrange equation.

In this paper, we demonstrate the existence of multiple length scale wave propagation in a Belousov–Zhabotinsky (BZ) reaction–transport (i.e., diffusion) system. By varying the concentration of bromate to modulate the dynamics of the

propagation medium, we are able to observe not only period-doubled propagation, but also bursting behavior. The experimental results, which are qualitatively reproduced by numerical simulations of a five-variable Oregonator model, suggest a general mechanism for generating multiscale structures via the depletion of key species during the production of phase waves in a system with concentration gradients.

Unidirectional wave propagation has been reported previously by Yoshida et al. for free narrow strips of a gel that incorporates the catalyst of the BZ reaction and is immersed in a solution of the reactants.^{10–12} In our work, we change the boundary conditions by placing the gel in a capillary that has one end sealed and the other end open, which can be placed in contact with a solution containing the BZ reactants. The reactants thus flow unidirectionally toward the closed end of the capillary. Pulse waves of oxidation can initiate spontaneously and repeatedly at the open end and then propagate toward the closed end, as shown in Figure 1. Concentration changes in the BZ reaction can be monitored by the color change of the Ru(bpy)₃ catalyst.¹³ Pale blue and orange regions indicate oxidized and reduced states, respectively. The oscillatory mechanism of the BZ reaction has been studied extensively,¹⁴ and we employ a mechanistically based model, described in the Simulation Section, to simulate the

Received: October 1, 2013

Accepted: November 1, 2013

Published: November 1, 2013

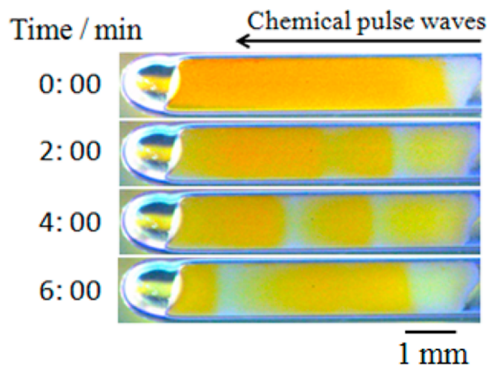


Figure 1. Unidirectional propagation of chemical pulse waves in a one-dimensional BZ gel system. Waves appear as pale blue bands. Concentrations of external solution: $[HNO_3]_0 = 0.90\text{ M}$, $[MA]_0 = 63\text{ mM}$, $[NaBrO_3]_0 = 72\text{ mM}$. Composition of the polymer is given in the Experimental Section.

propagation of pulse waves in our capillary. The space-time plots of our experiments and simulations presented in Figures 2–5 depict the propagation of pulse waves in our capillary. They describe the evolution of pulse-lengths in time, much as Meinhardt¹⁵ explains the development of patterns on sea shells, where the passage of time is reflected in the growth direction of the pattern.

Yamaguchi et al. reported temporal evolution of spiral patterns in two-dimensional BZ silica gels containing ferroin catalyst, noting that the patterns tend to become regular as the reactants within the gel become more uniform.¹⁶ In our experiment with a capillary open at one end, space-time plots were constructed by lining up one-dimensional images along the central axis of the capillary. As we see in Figure 2, chemical pulse waves originate spontaneously at the right open end and propagate toward the closed left end. The propagation scale exhibits period-doubling bifurcation, starting from P^1 (simply periodic) and evolving to P^2 , P^4 , and P^8 (spatial periods 2, 4, and 8, respectively) with time, as shown in Figure 2a,b. Then the chemical pulse waves transform to P^{16} (Figure 2c). At somewhat longer times, we observe a stable P^{16} state shown in Figure 2d,e. This last propagation mode persists for much of the duration of the experiment (nearly 12 h). We therefore define this state as the characteristic pulse wave under these experimental conditions. Finally, the pattern fades as a result of degradation of the Ru-complex (Figure 2f,g). The simulations in Figure 3 based on the five-variable Oregonator model¹⁷ are in good agreement with these experimental observations.

Complex oscillations and chaos have been observed previously in homogeneous BZ reaction mixtures.³ Wave propagation in a diffusion-fed system can be tuned by varying the reservoir concentrations of the reactants diffusing into the tube filled with BZ gel. As we see in Figure 4a–g, the space-time structure for the propagation length of characteristic pulse waves becomes more complex as $[NaBrO_3]_0$ is increased, changing from bursting to P^1 , P^2 , P^4 , P^8 , and P^{16} , and finally to a mixture of oxidized steady state (refractory state) and pulse waves. Our results demonstrate that the concentration of bromate can be used as a control parameter for the bifurcations that lead to multiple length scale propagation. We obtain the same bifurcation sequence in simulations with our five-variable reaction-diffusion model, as shown in Figure 5.

The frequency of the pulse waves initiated at the open end increases with $[NaBrO_3]_0$ both in the experiments and the simulations (Figure 4 and 5). Each propagating pulse in a wave train follows the preceding pulse. When $[NaBrO_3]_0$ is low, a sequence of pulses (two in Figure 4a and 5a, three in Figure 5b) depletes the bromate enough so that extra time is required to allow propagation of the next set of pulses, resulting in bursting. At somewhat higher bromate concentration, the medium can recover sufficiently after each pulse, and successive waves propagate into a medium with the same concentration amplitude and therefore have the same propagation length (P^1 propagation mode, Figure 4b). When we increase $[NaBrO_3]_0$ further, the interval between successive pulse waves decreases (Figure S1 in the Supporting Information). Now the concentration of inhibitor after a pulse remains elevated for the following pulse. As a result, the concentration amplitude of the following pulse decreases and is insufficient to support each pulse wave propagating an equal distance. The new big pulse near the closed end can recover after a shorter pulse, so we have an alteration of pulse lengths. Detailed concentration profiles obtained from a numerical simulation are shown in Figure 6. The preceding wave leaves an inhibitory maximum in $W([Br^-])$, which causes annihilation of the subsequent wave. Without enough time after the preceding pulse, the concentration of inhibitor cannot drop sufficiently far, resulting in multiple propagation lengths of the pulse waves.

We further performed experiments to investigate the behavior of a stirred bulk solution with the same concentrations of BZ species as in the gel. Corresponding to period-8 length scale pattern formation, the experimental result demonstrates that only simple oscillations occur in the bulk solution, as shown in the Supporting Information (see Figure S2).

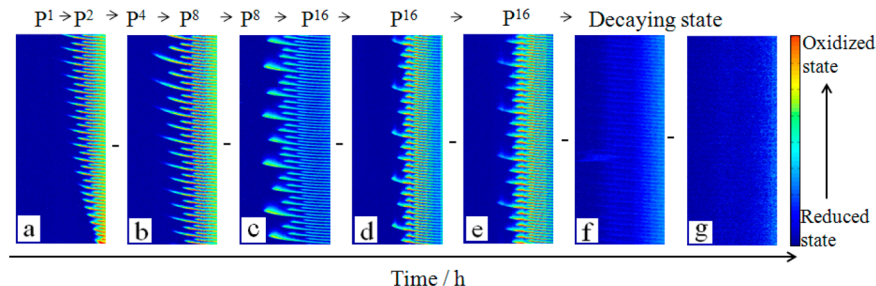


Figure 2. Time evolution of pulse waves propagating from right to left in a pseudo-one-dimensional BZ gel system. Horizontal and vertical axes indicate space and time, respectively, for each frame, with time increasing upward. Each space-time plot consists of 2000 horizontal data scans along the center axis of the BZ gel in the capillary at 5 s intervals (i.e., the span of each space-time plot is 2.78 h). Starting time of each frame: (a) 0 h, (b) 2.78 h, (c) 6.26 h, (d) 9.16 h, (e) 17.98 h, (f) 21.53 h, and (g) 25.46 h. Concentrations of solutions: $[HNO_3]_0 = 0.90\text{ M}$, $[MA]_0 = 63\text{ mM}$, $[NaBrO_3]_0 = 72\text{ mM}$.

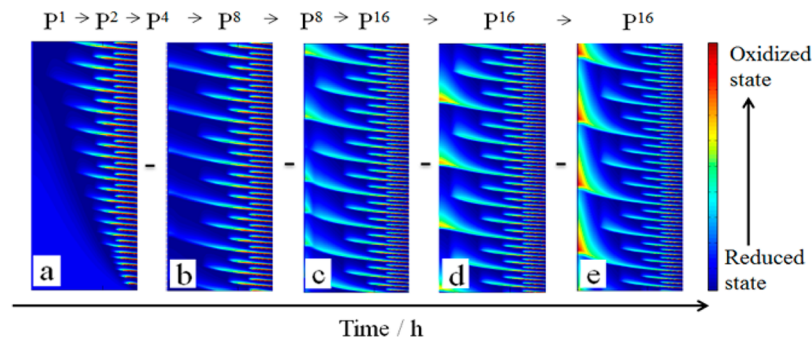


Figure 3. Simulated space-time plots of pulse waves propagating in a pseudo-one-dimensional BZ gel system. The system consists of 1024 grid points (length = 5 mm); grid spacing: $\Delta x = 4.888 \times 10^{-4}$ cm; time step: $\Delta t = 10^{-3}$ s; diffusion coefficients: $D_A = D_B = 3.624 \times 10^{-6}$ cm 2 /s, $D_U = D_W = 7.248 \times 10^{-6}$ cm 2 /s, $D_V = 0.0$ (the catalyst was immobilized in the gel); initial concentration of $V = 10^{-5}$ M throughout the gel; other initial concentrations were set to zero except at the grid point at the right boundary ($x = 0.0$ mm); Dirichlet boundary conditions were used at the right boundary with $H_0 = 0.90$ M, $A_0 = 37.9$ mM, $B_0 = 63$ mM, $U_0 = V_0 = W_0 = 0.0$ M; each plot consists of 1500 data points at 5 s intervals (i.e., the span of each space-time plot is 2.08 h). Starting time of each frame: (a) 0 h, (b) 2.08 h, (c) 18.05 h, (d) 25.00 h, (e) 50.00 h.

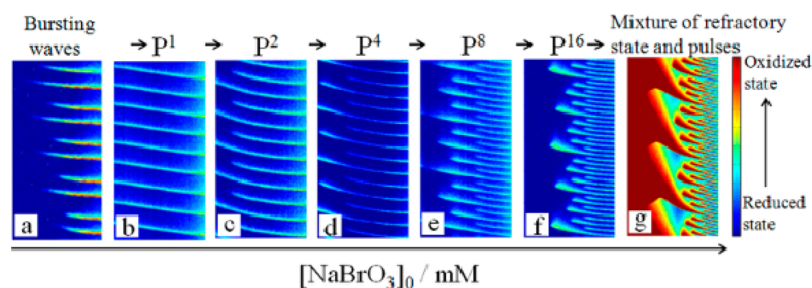


Figure 4. Space-time plots showing multiple length scale instability of characteristic pulse propagation as a function of $[NaBrO_3]_0$. Each plot consists of 800 horizontal data points extracted along the center axis of the BZ gel at 5 s intervals (time-span of each space-time plot is 1.11 h). $[NaBrO_3]_0$ = (a) 32 mM, (b) 36 mM, (c) 46 mM, (d) 54 mM, (e) 60 mM, (f) 72 mM, and (g) 112 mM. $[HNO_3]_0 = 0.90$ M, $[MA]_0 = 63$ mM.

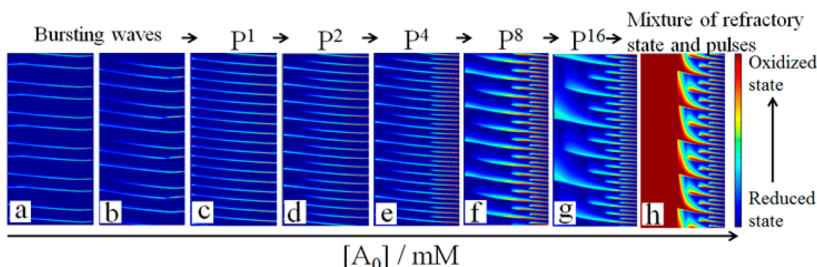


Figure 5. Simulated space-time plots showing multiple length scale instability of characteristic pulse propagation as a function of A_0 . Each plot consists of 1000 data points at 5 s intervals (time-span of each space-time plot is 1.42 h). $[A_0]$ = (a) 11.8 mM, (b) 12.06 mM, (c) 12.1 mM, (d) 13.3 mM, (e) 24.4 mM, (f) 37.0 mM, (g) 37.9 mM, and (h) 41.8 mM. Other parameters are as in Figure 3.

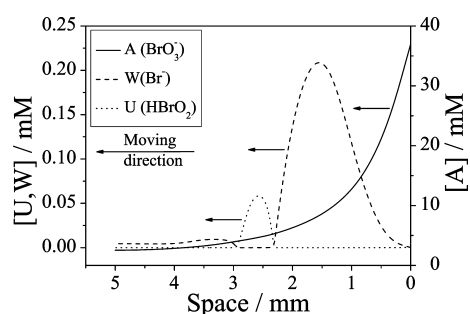


Figure 6. Concentration profiles of variables A (BrO_3^-), U (Br^-), and W ($HBrO_2$) from the simulated period-8 propagation pulses at time = 20,100 s with parameters and travel direction of waves as in Figure 5f.

Compared with the simple homogeneous oscillations, points in the gel display quite different local dynamics, as quantified by

the time series of gray levels shown in Figure 7. The figure demonstrates that, as we move away from the open end, the local oscillatory mode is transformed from P^8 , P^4 , P^2 , to P^1 , and the period increases with the distance from the open end, since a decreasing fraction of the pulses reaches the more distant regions of the capillary (Figure 4e). We see in Figure 7 that point a is the closest point to the bulk solution, where the concentration of bromate is highest. The dissipation of reactants with distance from the feeding end produces a continuous drop in the bromate concentration, which increases the local oscillatory period and yields simple oscillations, as shown in Figure 8d, near the far end of the capillary. This simulated sequence of local dynamics along the capillary agrees well with the experimental results (cf. Figures 7 and 8).

A homogeneous reaction under our experimental conditions, in which all reactants have the same concentrations as in the reservoir solutions, displays oscillations (e.g., Figure S2 in the

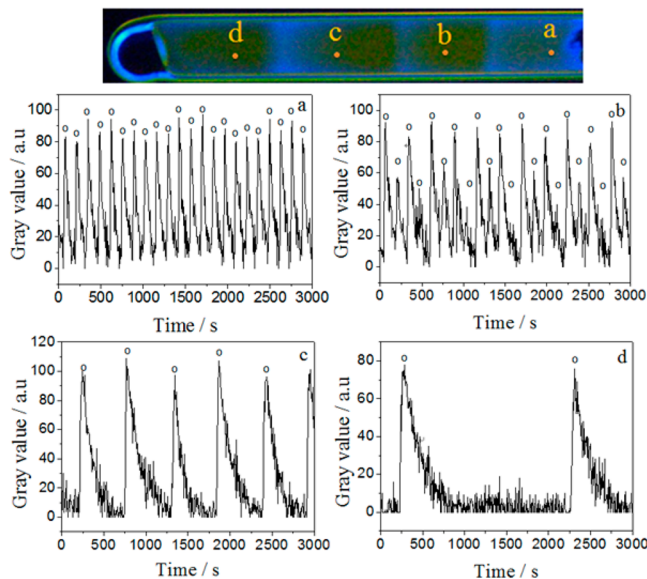


Figure 7. Oscillations of gray level (proportional to concentration of oxidized catalyst) at different points in a capillary filled with BZ gel. Experimental parameters and conditions as in Figure 4e.

Supporting Information), a necessary condition for phase waves. On the other hand, the delivery of reactants (e.g., bromate) and their reactive consumption lead to a persistent gradient in reactant concentration along the tube, as shown in Figure 6, resulting in gradients of both frequency and phase, producing unidirectional phase waves, i.e., the high frequency oscillations at the open end of the tube determine the propagation direction of the waves,^{18–21} similar to those seen with micropatterning chemical oscillations in the Brigg–Rauscher system where a transient frequency gradient leads to phase waves.²² In our system, the reservoir reactants (BrO_3^- , H^+ , and MA) diffuse with fixed concentrations into the capillary from the open end, ensuring a nearly constant gradient of

species concentrations and steady spatiotemporal structures that can be maintained until the Ru-complex begins to degrade after more than 20 h. The above two characteristics of our system (oscillatory medium and persistent concentration gradient) suggest that the waves are driven by a persistent phase gradient. The decrease of bromate concentration along the tube leads to both an increase in the local oscillation period and a gradual decrease of the local oscillation amplitude, producing pulse waves with multiple length scales.

We have observed multiple length scale instabilities, i.e., period doubling and bursting, resulting from the coupling of reaction and diffusion, in the wave propagation distance in both experiments on a diffusion-fed pseudo-one-dimensional BZ gel and numerical simulations of a five-variable Oregonator model. An obvious feature of the diffusion-fed system is that those instabilities are induced by diffusion, since only simple oscillations occur in a stirred solution with the same composition as the gel reaction in both experiment and simulation. Gorecki and co-workers have studied related phenomena in a FitzHugh–Nagumo-type model of chemical pulses passing through a passive barrier between two excitable media.²³ They find that the fraction of pulses able to pass through the barrier varies with the width of the barrier and the time between pulses. In a related set of experiments and simulations of a three-variable Oregonator model,²⁴ they observe period-doubling as a function of the illumination intensity in the depth of penetration of pulses in a dark triangular excitable BZ medium surrounded by an illuminated nonexcitable region.

The phenomena observed here and growth patterns in nature display similar regularities and may arise from common dynamical sources. In growing plants, for example, the roots are open to diffusion of water and nutrients only at one end, as in our capillary geometry. The pulse waves studied in this work were limited to essentially a single spatial dimension, while many natural multiple length scale patterns are two- and three-dimensional. We hope that this work will inspire further

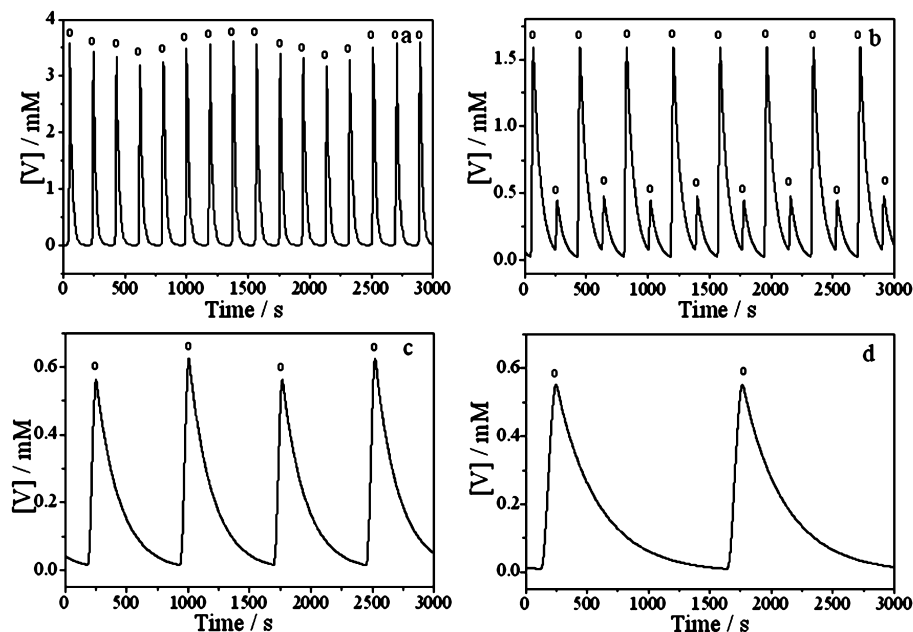


Figure 8. Local oscillations of variable V at different grid points for the simulated period-8 length scale of propagation pulses. (a) $x = 4.888 \times 10^{-2}$ mm, (b) $x = 1.134$ mm, (c) $x = 3.421$ mm, (d) $x = 4.643$ mm. Other parameters and conditions as in Figure 5.

investigations to understand the more complex multiple length scale patterns that arise in higher-dimensional media.

■ EXPERIMENTAL SECTION

In order to obtain a pseudo-one-dimensional BZ gel, we used a glass capillary of inner diameter 1.0 ± 0.1 mm as a synthetic template in accordance with previous work.²⁵ *N*-isopropyl acrylamide (NIPAAm, Tokyo Chemical Industry Co., Inc.), 2,2'-azobis (isobutyronitrile) (AIBN, Sigma-Aldrich), *N,N'*-methylenebisacrylamide (MBAAm, Sigma-Aldrich), and 2-acrylamido-2-methylpropanesulfonic acid (AMPS, Sigma-Aldrich) were purified by recrystallization before use. 2,2-dipyridyl (Sigma-Aldrich), 4,4'-dimethyl-2,2'-dipyridyl (Sigma-Aldrich), and ruthenium(III)chloride (Sinopharm Chemical Reagent Co., Inc.) were reagent grade chemicals and were used without purification. Ruthenium(4-vinyl-4'-methyl-2,2'-bipyridine)bis(2,2'-bipyridine)bis(hexafluorophosphate) (Ru(vm-bpy)(bipy)₂(PF₆)₂) was synthesized according to established protocols.^{26,27}

NIPAAm (0.305 g), Ru(vm-bpy)(bipy)₂(PF₆)₂ (37.8 mg), and MBAAm (3.5 mg) were dissolved in 1.0 mL of methanol, and AMPS (10.2 mg) was dissolved in 1.0 mL of distilled water (both the methanol and water were previously purged with nitrogen gas). The two solutions were mixed and injected into the glass capillary, which was sealed with PVC, and then polymerized at 60.0 °C for 24 h. After gelation, the capillary was cut into small sections (5.0 mm in length). The resulting BZ gel was soaked in pure methanol for a week to remove unreacted monomers, and then gradually hydrated¹⁰ to yield the final pure pseudo-one-dimensional poly(NIPAAm-*co*-Ru(bpy)₃-*co*-AMPS) gel. The characterization of the BZ gel is given in the Supporting Information (Figure S3). Since conventional poly(NIPAAm-*co*-Ru(bpy)₃-*co*-AMPS) gels can undergo periodic swelling and shrinking when coupled to the BZ reaction (10,11), we doubled the normal dosage of cross-linker (MBAAm) to eliminate the chemoresponsiveness of the gel (see Supporting Information and Figure S4) so that the only effects observed arose from reaction-diffusion.

The resulting BZ gel in a capillary with one open end was immersed in 8 mL of a catalyst-free BZ solution containing malonic acid (MA, 63 mM), nitric acid (HNO₃, 0.90 M), and sodium bromate (NaBrO₃, 20–108 mM), which were reagent-grade chemicals without further purification. The temperature of the solution was maintained at 20.0 °C. The pulse waves initiated spontaneously at the open end. The patterns were recorded with a charge-coupled-device (CCD) camera (TUSEN, TCC-1.4CHICE) connected to a computer. A halogen light source provided monochromatic light through a blue filter ($\lambda_{\text{max}} = 455$ nm). Space-time plots along the central axis of the capillary were constructed to analyze the propagating waves, and local concentrations of oxidized catalyst were measured as gray levels. The image capture system is described in the Supporting Information (see Figure S5).

■ SIMULATION SECTION

A five-variable Oregonator model was used to simulate the reaction-diffusion waves:^{16,28}

$$\begin{aligned}\frac{\partial A}{\partial t} &= D_A \frac{d^2 A}{dx^2} - k_1 AW - k_3 AU + k_4 U^2 \\ \frac{\partial B}{\partial t} &= D_B \frac{d^2 B}{dx^2} - k_5 BV \\ \frac{\partial U}{\partial t} &= D_U \frac{d^2 U}{dx^2} + k_1 AW - k_2 UW + k_3 AU - 2k_4 U^2 \\ \frac{\partial V}{\partial t} &= 2k_3 AU - k_5 BV \\ \frac{\partial W}{\partial t} &= D_W \frac{d^2 W}{dx^2} - k_1 AW - k_2 UW + h k_5 BV\end{aligned}$$

where A , B , U , V , and W correspond to the concentrations of BrO₃⁻, BrMA, HBrO₂, Ru(bpy)₃³⁺ and Br⁻, respectively. D_x is the diffusion coefficient of the corresponding species. Following the work of Kettunen et al.,²⁸ in which they observed transient states of period-doubling propagation waves, we use this five-variable model to reproduce our experimental period-doubling and bursting instabilities in the spatial extent of wave propagation. The PDEs were numerically integrated using an explicit fourth-order Runge-Kutta method and utilizing three-point central-difference approximations for the 1D Laplacian operators. For our gel reaction-diffusion system with diffusive feeding from the open end, Dirichlet, and zero-flux boundary conditions were used at the open and sealed ends, respectively. The kinetic parameters were chosen from work by Tyson¹⁷ and Kettunen:²⁸ $k_1 = 2.0 \times [H^+]^2 M^{-3}s^{-1}$, $k_2 = 1.0 \times 10^6 [H^+] M^{-2}s^{-1}$, $k_3 = 40.0 \times [H^+] M^{-2}s^{-1}$, $k_4 = 2.0 \times 10^3 M^{-1}s^{-1}$, $k_5 = 0.95 M^{-1}s^{-1}$, $[H^+] = 0.90 M$ and $h = 0.9$. D_v was set to zero, because the catalyst is immobilized in the gel.

■ ASSOCIATED CONTENT

Supporting Information

(A) Dependence of interval between successive pulse waves on [NaBrO₃]₀. (B) Experimental and simulated oscillations in bulk solution. (C) SEM of the BZ gel. (D) Effect of concentration of cross-linker on chemoresponsiveness of the gel. (E) Schematic diagram of image capture system. This material is available free of charge via the Internet at <http://pubs.acs.org>.

■ AUTHOR INFORMATION

Corresponding Authors

*E-mail: epstein@brandeis.edu (I.R.E.).

*E-mail: gaoqy@cumt.edu.cn (Q.G.).

Notes

The authors declare no competing financial interest.

■ ACKNOWLEDGMENTS

This work was supported in part by Grants No. 21073232 and S1221462 from the National Natural Science Foundation of China, the Fundamental Research Funds for the Central Universities (No. 2013XK05) and PAPD. I.R.E. acknowledges Grant No. CHE-1012428 from the U.S. National Science Foundation.

■ REFERENCES

- (1) Epstein, I. R.; Pojman, J. A. *An Introduction to Nonlinear Chemical Dynamics: Oscillations, Waves, Patterns, and Chaos*; Oxford University Press: New York, 1998.

- (2) Balanov, A.; Janson, N.; Postnov, D.; Sosnovtseva, O. *Synchronization: From Simple to Complex*; Springer-Verlag: Berlin, 2009.
- (3) Scott, S. K. *Chemical Chaos*; Oxford University Press: New York, 1991.
- (4) Nelson, T.; Dengler, N. Leaf Vascular Pattern Formation. *Plant Cell* **1997**, *9*, 1121–1135.
- (5) Kücken, M.; Newell, A. C. A Model for Fingerprint Formation. *Europhys. Lett.* **2004**, *68*, 141–146.
- (6) Cerdá, E.; Mahadevan, L. Geometry and Physics of Wrinkling. *Phys. Rev. Lett.* **2003**, *90* (074302), 1–4.
- (7) Losert, W.; Shi, B. Q.; Cummins, H. Z.; Warren, J. A. Spatial Period-doubling Instability of Dendritic Arrays in Directional Solidification. *Phys. Rev. Lett.* **1996**, *77*, 889–891.
- (8) Warren, J. A.; Langer, J. S. Prediction of Dendritic Spacings in a Directional Solidification Experiment. *Phys. Rev. E* **1993**, *47*, 2702–2712.
- (9) Brau, F.; Vandeparre, H.; Sabbah, A.; Pouillard, C.; Bouadaoud, A.; Damman, P. Multiple-Length-Scale Elastic Instability Mimics Parametric Resonance of Nonlinear Oscillators. *Nat. Phys.* **2011**, *7*, 56–60.
- (10) Maeda, S.; Hara, Y.; Sakai, T.; Yoshida, R.; Hashimoto, S. Self-Walking Gel. *Adv. Mater.* **2007**, *21*, 3480–3484.
- (11) Murase, Y.; Maeda, S.; Hashimoto, S.; Yoshida, R. Design of a Mass Transport Surface Utilizing Peristaltic Motion of a Self-Oscillating Gel. *Langmuir* **2009**, *1*, 483–489.
- (12) Yoshida, R.; Kokufuta, E.; Yamaguchi, T. Beating Polymer Gels Coupled with a Nonlinear Chemical Reaction. *Chaos* **1999**, *2*, 260–266.
- (13) Degn, H. Oscillating Chemical Reactions in Homogeneous Phase. *J. Chem. Educ.* **1972**, *5*, 302–307.
- (14) Field, R. J.; Körös, E.; Noyes, R. M. Oscillations in Chemical Systems. II. Thorough Analysis of Temporal Oscillation in the Bromate–Cerium–Malonic Acid System. *J. Am. Chem. Soc.* **1972**, *94*, 8649–8664.
- (15) Meinhardt, H. *The Algorithmic Beauty of Sea Shells*; Springer: Berlin, 2009.
- (16) Yamaguchi, T.; Kuhnert, L.; Nagy-Ungvarai, Z.; Müller, S.; Hess, B. Gel Systems for the Belousov–Zhabotinskii Reaction. *J. Phys. Chem.* **1991**, *15*, 5831–5837.
- (17) Tyson, J. J.; Fife, P. C. Target Patterns in a Realistic Model of the Belousov–Zhabotinskii Reaction. *J. Chem. Phys.* **1980**, *73*, 2224–2237.
- (18) Mikhailov, A. S.; Engel, A. Multiple Target Pattern Creation and Synchronization Phenomena. *Phys. Lett. A* **1986**, *117*, 257–260.
- (19) Blasius, B.; Tönjes, R. Quasiregular Concentric Waves in Heterogeneous Lattices of Coupled Oscillators. *Phys. Rev. Lett.* **2005**, *95* (084101), 1–4.
- (20) Bordiougov, G.; Engel, H. From Trigger to Phase Waves and Back Again. *Phys. D (Amsterdam, Neth.)* **2006**, *215*, 25–37.
- (21) Kheowan, O. U.; Mihaliuk, E.; Blasius, B.; Sendina-Nadal, I.; Showalter, K. Wave Mediated Synchronization of Nonuniform Oscillatory Media. *Phys. Rev. Lett.* **2007**, *98* (074101), 1–4.
- (22) Bishop, M. K. J.; Fialkowski, M.; Grzybowski, B. A. Micropatterning Chemical Oscillations: Waves, Autofocusing, and Symmetry Breaking. *J. Am. Chem. Soc.* **2005**, *127*, 15943–15948.
- (23) Sielewiesuk, J.; Górecki, J. Complex Transformations of Chemical Signals Passing through a Passive Barrier. *Phys. Rev. E* **2002**, *66* (016212), 1–9.
- (24) Kitahata, H.; Fujio, K.; Gorecki, J.; Nakata, S.; Igarashi, Y.; Gorecka, A.; Yoshikawa, K. Oscillation in Penetration Distance in a Train of Chemical Pulses Propagating in an Optically Constrained Narrowing Channel. *J. Phys. Chem. A* **2009**, *115*, 10405–10409.
- (25) Yoshida, R.; Otoshi, G.; Yamaguchi, T.; Kokufuta, E. Traveling Chemical Waves for Measuring Solute Diffusivity in Thermosensitive Poly(*N*-isopropylacrylamide) Gel. *J. Phys. Chem. A* **2001**, *105*, 3667–3672.
- (26) Ghosh, P.; Spiro, T. G. Photoelectrochemistry of Tris(bipyridyl)ruthenium (II) Covalently Attached to n-Type Tin (IV) Oxide. *J. Am. Chem. Soc.* **1980**, *17*, 5543–5549.
- (27) Schultze, X.; Serin, J.; Adronov, A.; Fréchet, J. M. J. Light Harvesting and Energy Transfer in a Ruthenium–Coumarin-2 Copolymer. *Chem. Commun.* **2001**, *13*, 1160–1161.
- (28) Kettunen, P.; Yamaguchi, T.; Hashimoto, H.; Amemiya, T.; Steinbock, B.; Müller, S. C. Emergent Reaction–Diffusion Phenomena in Capillary Tubes. *Chaos* **2006**, *16* (037111), 1–7.